Integration of a luminescent solar concentrator: Effects on daylight, correlated color temperature, illuminance level and color rendering index

Niccolò Aste [a], Lavinia Chiara Tagliabue [a,*], Pietro Palladino [a], Daniele Testa [b]

[a] *Architecture, Built environment and Construction Engineering Department – Politecnico di Milano, via Bonardi 9, 20133 Milan, Italy*
[b] *Eni S.p.A, Research Center for Non-Conventional Energies – Istituto ENI Donegani, Research and Technological Innovation Department, via Giacomo Fauser, 4, 28100 Novara, Italy*

Received 7 May 2014; received in revised form 15 December 2014; accepted 29 January 2015
Available online 20 February 2015

1. Introduction

Luminescent Solar Concentrators (LSCs) are solar active devices (Goetzberger and Greubel, 1977; Goetzberger, 1978; Swartz et al., 1977) that can be suitable to be integrated in architecture (Van Sark, 2013), preserv-ing transparency of the envelope and therefore assuring profitable energy production and light exploitation into the building spaces. The interest in LSC comes from the opportunity to reduce the photovoltaic surface, which is located only on the edges of the component, and the related costs and to improve daylighting into the indoor spaces. Office buildings are often realized with wide transparent façades, causing in many cases glare and overheating problems to the users (Nazzal, 2005; Fadzil and Sia, 2004; Kim and Kim 2012; Shin et al., 2012). However the architectural language seems to be unavoidable connected to the transparent image of this kind of the buildings in which shading systems, to control and manage the daylight, have to be considered even into the design phase. LSCs can be applied as part of the transparent envelope paying attention to the color due to the dyes dispersed into the plastic bulk used. When transparency and a more extensive use of diffuse

* Corresponding author. Tel./fax: +39 02 2399 9469.
E-mail address: chiara.tagliabue@polimi.it (L.C. Tagliabue).

Nomenclature

Variables and parameters

λ	wavelength (nm)
V	luminous efficiency (–)
$V(\lambda)$	photopic function (nm)
K	luminous efficacy (lm/W)
E	illuminance (lx)
Φ	flux (W, lm)
UGR	unified glare rating (–)
R_a	general color rendering index (–)
$R1$ to $R15$	special color rendering indexes (–)
CCT	correlated color temperature (K)
SPD	spectral power distribution (W/m^2 nm)
τ	transmission coefficient (–)

Subscript

λ	spectral
m	average value
min	minimum value
v	visible
e	radiant
CG	clear glass
LSC	luminescent solar concentrator

radiation are required, LSCs components may be a good alternative to traditional photovoltaic systems (Wiegman and Van Der Kolk, 2012). However their durability and technical–economic competitiveness have to be ensured (Debije and Verbunt, 2012).

This paper describes the first daylighting evaluations carried out on a new LSC prototype, developed by ENI Donegani Institute (Scudo et al., 2010) and analyzed by Politecnico di Milano, in which photoluminescent dyes are dispersed into a polymethylmethacrylate (PMMA) sheet. The dyes developed in the first research phase and dispersed in the plastic transparent slab provide a yellow color to the component. Photovoltaic performances have been dealt with in other studies.

The dyes dispersed in the transparent slab are: DTB (4,7-di(2-thienyl)benzo[c]1,2,5-thiadiazole) synthesized by ENI, and DPA (9,10-diphenylanthracene), a commercial dye (Patent Number(s): WO2011048458-A1; WO20110 48458-A8) (Aste et al., 2015). The curves of absorption and photoluminescent intensity of emission related to the two dyes are shown in Fig. 1.

Experimental measurements on the absorption and emission spectra of DPA and DTB dyes, carried out at ENI Donegani Institute, are represented in Fig. 1. The two parameters are defined below.

Absorbance is the logarithmic ratio of the amount of radiation falling upon a material to the amount of radiation transmitted through the material. Absorbance at a certain wavelength of light (λ), denoted A_λ, is a quantitative measure expressed as:

$$A_\lambda = \log_{10}\frac{I_0}{I}$$

i.e., as an unsigned logarithmic ratio between I_0, the radiation falling upon a material (the intensity of the radiation before it passes through the material or incident radiation) and I, the radiation transmitted through a material (the intensity of the radiation that has passed through the material or transmitted radiation).

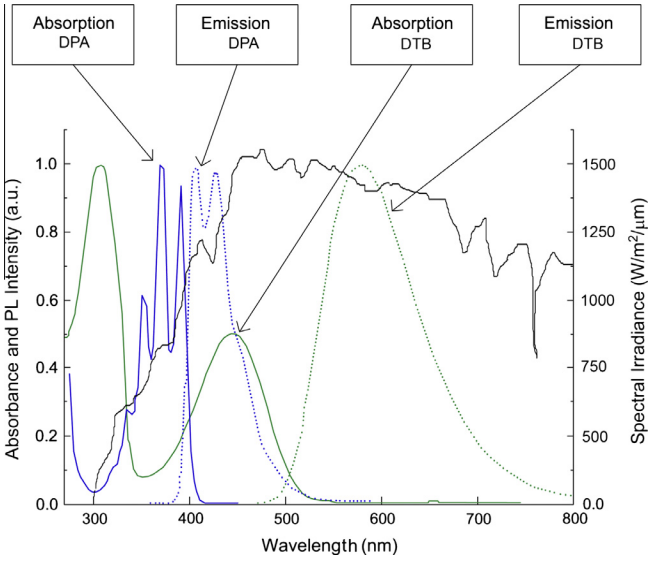

Fig. 1. Absorbance and emission spectra of DTB and DPA and Solar spectrum (Air Mass 1.5);.

Photoluminescence Intensity is the ratio between emitted and absorbed photons, expressed also as fluorescence quantum yield ($\Phi_{PL} = 0.83$ for DPA and $\Phi_{PL} = 0.90$ for DTB).

The yellow LSC component can be integrated in different parts of the building envelope carefully considering the color affection on visual comfort parameters (Lynn et al., 2012; Palladino, 2005; Palladino 2002; Coppedè and Palladino 2012).

The integration of the yellow LSC changes the quality of light in the indoor space, the light becomes warmer as the correlated color temperature (CCT) is lowered in comparison with a clear glass solution. The decrease of the CCT produces favorable effects on visual comfort and can enhance the cold light in climates in which covered sky are prevailing. Moreover the color of the dyes produces a spectral shifting of the wavelength that comes closest to

the human visible peak wavelength in the photopic vision, improving the illuminance level and luminous efficacy of the light in the indoor spaces, as described in Section 5.

2. Parameters of luminous performance

The quantity of light is the first parameter which should be controlled in the luminous performance analysis and it is quantified through the illuminance level E [lx] that is the luminous flux Φ_v [lm] reaching a point on a surface [m^2].

The sensitivity of human vision system is connected to the wavelength of light (Tachibanaki et al., 2007; Petrides and Trexler, 2008; Fekete et al., 2010), and the spectral eye sensitivity curve $V\lambda$ has the peak wavelength at 555 nm. The wavelength and color of the light regulates biological effects of the light–darkness cycle too (Berson et al., 2002; Hattar et al., 2002; Bellia et al., 2011; Dacey et al., 2005) influencing a large variety of bodily processes (Gamlin et al., 2007; Van Bommel, 2006) and playing an important role in governing alertness, sleep and therefore wellness (Morita et al., 2003; Webb, 2006). As a result the visual performance of the users in the indoor space is also related to quality of light (Linhart and Scartezzini, 2011) that means as primary factor the correlated color temperature CCT [K] which determinates the color of the light and thus the influence on the perception and wellness of the users and secondly the color rendering index R_a [–] which allows to perceive the natural color of the objects and to perform detailed visual tasks.

The international standard on lighting in working spaces requires the compliance of threshold values of a lim-ited number of variables specified for different activities. The main parameters indentified in the European Standard (EN 12646:2011) to quantify and qualify the correct light-ing in the workplaces are illuminance, CCT and R_a. The values of these parameters required in the work spaces range for illuminance between 200 and 750 lx, for CCT between 3000 K and 5300 K (i.e. warm and intermediate white light) and the value of R_a is 80 [–].

Thus the present study is focused on such parameters to assess the issue concerned, i.e. the effect of daylighting changed by a colored LSC component in the indoor space. For that reason the parameters assessed in the following analyses are the value of illuminance in a specific point and the CCT value, able to describe the effect of the LSC component in changing the quality of the incoming daylight.

The quantity of light (i.e. illuminance) and the quality of light (i.e. CCT) are the most relevant parameters to understand the possibility to reduce electrical needs in the indoor space and hence to achieve energy saving and to assess the quality of the environment perceived (Lutfi Hidayetoglu et al., 2012; Clements-Croome, 1977; Boyce and Cuttle 1990; Ju et al., 2012), moreover related to their correlation, affecting the users in performing medium or accurate visual tasks (Mills et al., 2007; Pinto et al., 2008). Finally, the col-or render index R_a, commonly used to evaluate the performance of artificial lighting, becomes interesting as a colored transparent surface is integrated into the building envelope and lot of cases can be found in which the color of the envelope is not previously evaluated in the design phase implying visual discomfort for the user and reduced capacity to perform detailed visual tasks.

3. Methodology

The appealing transparency and color of the LSC added to the photovoltaic generation make stronger the potential of such a component for building integration in façades and windows. For that reason it is crucial to analyze the LSC performance in term of daylighting exploitation.

The study start by considering that light can be exactly characterized by giving the radiative power of the source at each wavelength in the visible spectrum. The resulting spectral power distribution (SPD) contains all the basic physical data about the light and it is useful as starting point of color quantitative analyses. Accordingly, the analyses on the LSC sheet were carried out with a spectrometer on a scaled physic model of a single standard working space.

Therefore, a physical model of an office space with a glazed façade was realized and tested. The glazed façade was equipped with a main clear glazed window and a fanlight in which alternatively were tested a clear glass (light transmission $\tau_{v,CG} = 0.9$) and the yellow LSC sheet (light transmission $\tau_{v,LSC} = 0.75$).

The analyses were performed during an overcast day (10th January 2013 12 p.m., overcast sky illuminance $E_o = 3034$ lx) and a sunny day (28th May 2013 12 p.m., sunny sky illuminance $E_s = 70431$ lx) in Milan, Italy, evaluating the illuminance level and the CCT in the central point of the indoor space in the two façade configurations. Changes in the illuminance level and CCT were registered in the two sky conditions comparing the clear glazed façade with the LSC façade and during the sunny day expected problems of glare and color spot in the indoor space were highlighted.

Thus the same two configurations were tested with the addition to the physical model of a light-shelf located between the main window and the fanlight, to reflect direct upper light to the ceiling. This configuration allows avoiding the problem of color rendering, reducing possible problems of glare (Li, 2010; Hernandez-Andres et al., 1999, 2001; Van Bommel and Van den Beld, 2004), improving uniformity of illuminance by reducing light levels near the window (Littlefair, 1995; Soler and Oteiza, 1997) and enhancing them in the back of the room (Claros and Soler, 2002; Claros and Soler, 2001).

The measures were performed by a spectrometer which provides the distribution of SPD and the exact values of illuminance E and CCT.

4. Experimental set up

The paper reports the results in term of spectral power distribution (SPD), illuminance (E) and correlated color temperature (CCT) of the incoming light into a scaled physical model of an office space with the following façade configurations:

1. CG: clear glazed window and clear glazed fanlight;
2. LSC: clear glazed window and yellow LSC fanlight;
3. CG + LS: clear glazed window and clear glazed fanlight with the light shelf in between;
4. LSC + LS: clear glazed window and yellow LSC fanlight with the light shelf in between.

The analyzed façade was exposed to south to record the stronger effect due to direct solar radiation.

The scaled physical model has a clear glazed window sized 1/8 of the floor area with a fanlight in which a clear glass (CG) and the yellow LSC sheet (LSC) are placed alternatively. The first analysis was performed with these façade configurations, whereas a second step of analysis was performed with the addition of a light-shelf in the two configurations, i.e. without yellow LSC installed (CG + LS) and with LSC (LSC + LS). The model, openings and light-shelf dimensions are resumed in Table 1. The model is a 1:10 scaled model of the dimensions reported.

Table 1
Measures of the office space used as test cell through a 1:10 scaled physical model.

Dimensions	Length (m)	Width (m)	Height (m)
Office space	5.0	4.0	3.0
Working plan	–	–	0.85
Indoor space surfaces features	Ceiling	Walls	Floor
Reflective coefficient	0.7	0.5	0.3
Transparent window (clear glass)	2.0	–	1.2
Fanlight (clear glass or LSC)	2.0	–	0.5
Light-shelf	2.0	1.0	–

The experimental measures were performed with a spectrophotometer Konica Minolta CL 500A. The CL-500A can be used not only for illuminance measurements but also for spectral evaluation by using multiple sensors and an optical grating. The sensor based detector allows displaying spectral distribution in graphical form. Main

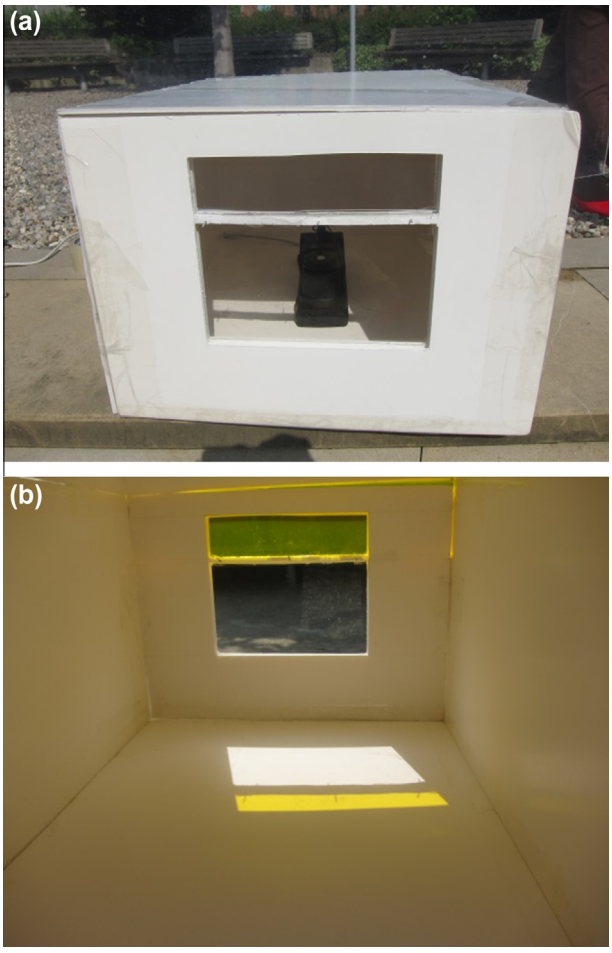

Fig. 2. Scaled physical model of the office space with the clear glass facade (CG) and internal view of the model with the yellow LSC fanlight (LSC). (For interpretation of the references to colour in this figure legend, the reader is referred to the web version of this article.)

Table 2
Specifications and error tolerances of the spectrophotometer CL-500A.

Specifications	
Model	Illuminance Spectrophotometer CL-500A
Illuminance meter class	Conforms to requirements for Class AA of JIS C 1609–11:2006 Illuminance meters Part 1: General measuring instruments Conforms to DIN 5032 Part 7 Class B
Spectral wavelength range	360–780 nm
Output wavelength pitch	1 nm
Spectral bandwidth	Approx. 10 nm (half bandwidth)
Wavelength precision	±0.3 nm (Median wavelength of 435.8 nm, 546.1 nm, and 585.3 nm as specified in JIS Z 8724
Measuring range	0.1 to 100,000 lx (chromaticity display requires 5 lx or more)
Accuracy (Standard Illuminant A)	E_v (illuminance):±2% ± 1 digit of displayed value
Visible-region relative spectral response characteristics (f_1')	Within 1.5% of spectral luminous efficiency $V(\lambda)$

specification and tolerance of the measurement instrument are collected in Table 2. Data recorded are processed by the instrument standard data management software CL-S10w. During the testing phase the spectrometer was located in the geometric center of the physical model.

In Figs. 2 and 3 are shown the façades configurations in the experimental setup.

Results of the measures are resumed and collected in the following Section 5.

5. Experimental measures on the physical scale model

Results in term of SPD, *E* and CCT were collected in overcast sky conditions (O) and in sunny sky condition (S) and compared to point out the variation on the light operated by the yellow LSC integrated into the south façade.

5.1. Experimental measures without light-shelf

Analyses in overcast conditions (i.e. CCT about 6500 K) (Judd et al., 1964) show that the installation of the yellow LSC reduces the illuminance level in the scaled model of about 20% and the CCT of a 24%, i.e. the illuminance value goes from 1811 lx to 1457 lx and CCT decreases from 4493 K with the clear glass to 3307 K with the yellow LSC. Therefore the integration of the yellow LSC makes the light warmer producing a pleasant and stimulating atmosphere with the CCT value ranging into the office space suitable values. In Fig. 4 spectral power distribution are plotted for the clear glass solution (CG) and the yellow fanlight solution (LSC) are plotted.

In sunny sky conditions the integration of the yellow LSC as fanlight allows an increase of the illuminance value by 11% i.e. the illuminance value goes from 10249 lx to 11499 lx. The correlated color temperature decreases by 23%, from 4021 K (i.e. white light intermediate) to 3277 K (i.e. light warm white).

It is possible to underline as the integration of the yellow LSC in the fanlight changes the color of the light towards higher wavelengths with a major power near the 560 nm.

In sunny sky condition the improvement of illuminance can be favorable however the daylighting levels of illuminance provided greatly exceed the lighting needs. The most significant advantage can be ascribed to the decrease of CCT which can enhance the perceptual and visual comfort (e.g. CCT for overcast sky is about 5500 K).

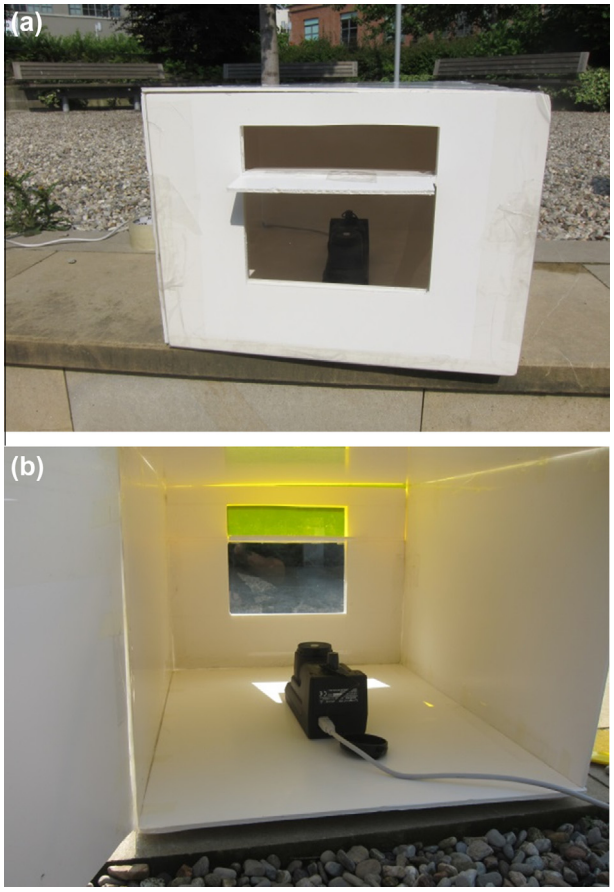

Fig. 3. Scaled physical model of the office space with the clear glass facade (CG + LS) and internal view of the model with the yellow LSC fanlight (LSC + LS). (For interpretation of the references to colour in this figure legend, the reader is referred to the web version of this article.)

5.2. Experimental measures with light-shelf

To overcome the problem of the color spot in the office space when direct radiation occurs (Fig. 1) a light-shelf was

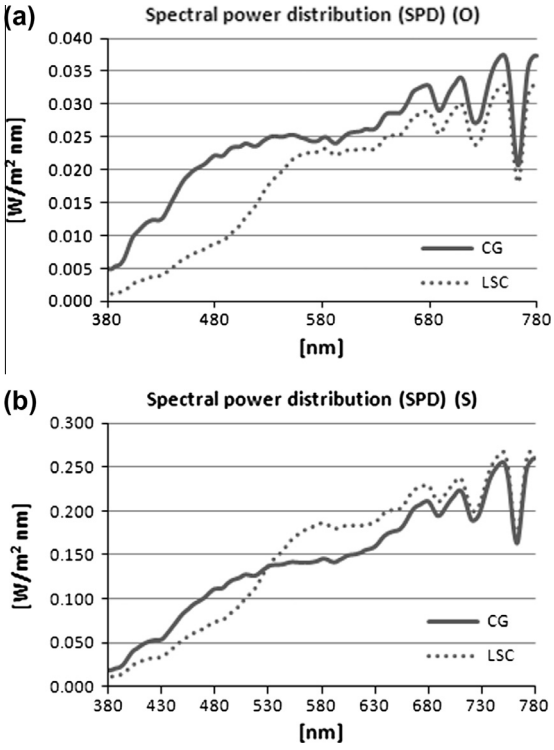

Fig. 4. Spectral power distribution (SPD) for the two configurations in overcast conditions (O) and in sunny sky condition (S).

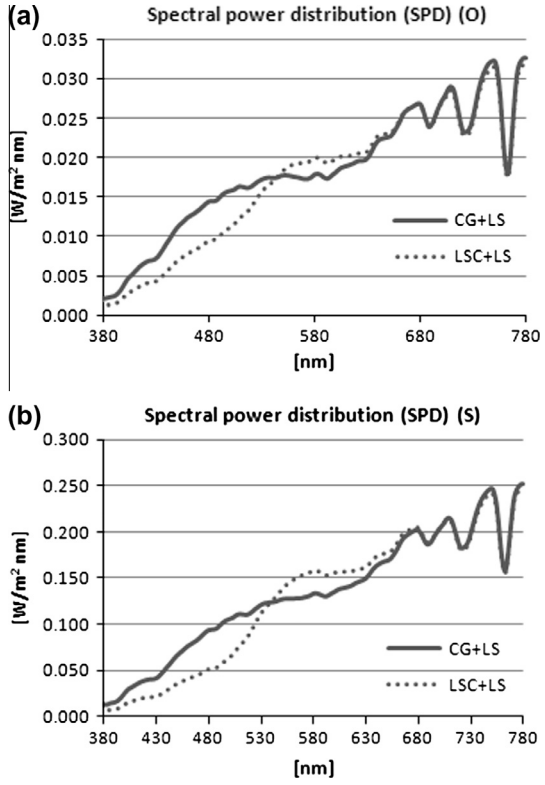

Fig. 5. Spectral power distribution (SPD): scaled physical model with light-shelf for the two configurations in overcast conditions (O) and in sunny sky condition (S).

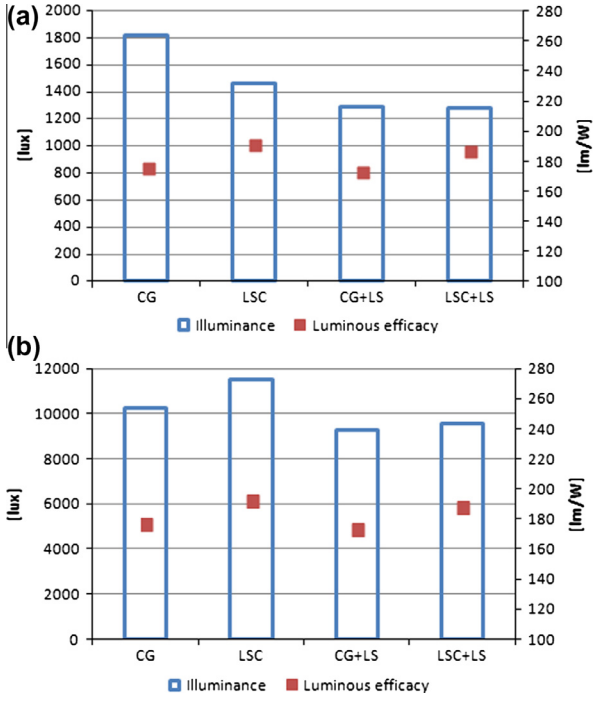

Fig. 6. Illuminance level E and luminous efficacy K of the LSC yellow plate installation in comparison with clear glass under overcast sky condition (a) and sunny sky condition (b).

added to reflect the yellow light to the ceiling and enhance the sunlight penetration into the room, shading the main window at the same time, thus reducing glare problems.

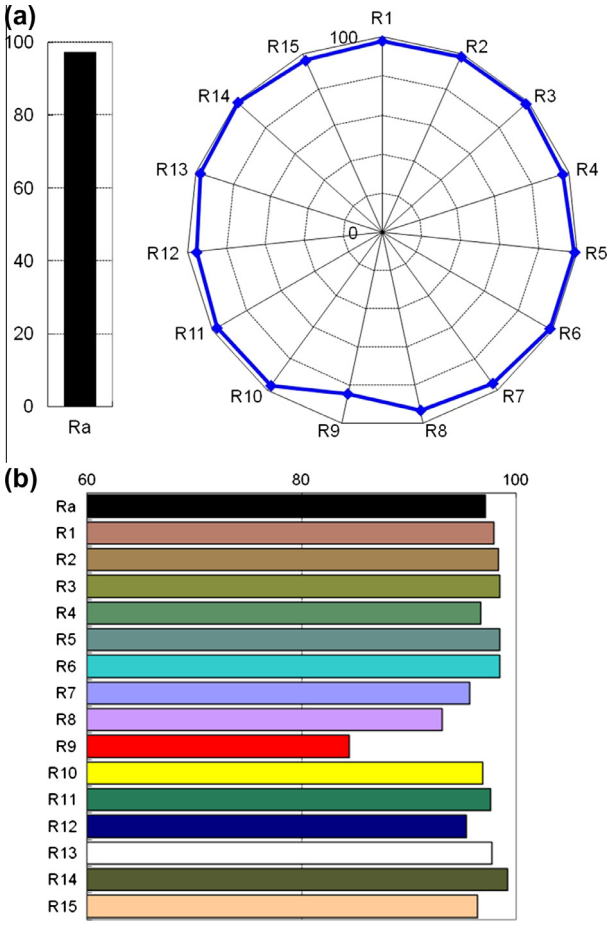

Fig. 7. Color rendering diagram of the scaled physical model with clear glass (CG). (For interpretation of the references to colour in this figure legend, the reader is referred to the web version of this article.)

From the previous figures of the model with and without the yellow LSC sheet it is possible to appreciate that the yellow light spot is avoided through the reflection operated by the light-shelf (Fig. 3). The ceiling reflects the yellowish light into the space and towards the back of the office space.

In Fig. 5 the spectral power distributions of the clear glass solution with the light-shelf (CG + LS) and of the façade integrating the LSC as fanlight with the light-shelf (LSC + LS) in overcast sky condition (O) and in sunny sky condition (S) are plotted.

Under overcast conditions the introduction of the light shelf is not strictly needed however this solution allows a major uniformity in illuminance distribution into the space. The situation with the light-shelf installed between the main window and the clear or yellow LSC fanlight showed no significant difference on illuminance level (i.e. a reduction of 0.2% with the LSC installation in comparison with the clear glass) and a decrease of CCT by 17% (i.e. from 4103 K to 3409 K) warming the overcast sky daylight.

In sunny sky condition, compared to the case without light-shelf, the addition of the shading system reduces the illuminance values in the indoor space of a 10% for the

clear glazed solution whereas for the LSC solution the reduction is about 17%. The improvement of the illuminance level between the clear glazed solution and the LSC integrated solution is confirmed however reduced to a 3%. The correlated color temperature changes for these two solutions from 3792 K (i.e. white light intermediate) to 3094 K (i.e. warm light) as in the previous case, with a reduction by 23%.

5.3. Comments on luminous efficacy

Evaluations on spectral luminous efficacy K defined as the ratio of luminous flux Φ_v [lm] to radiant spectral flux $\Phi_{e\lambda}$ [W], showed however that the yellow LSC installation (LSC, LSC + LS) produce a better result in comparison with the clear glass solution (CG, CG + LS) (i.e. an increment of 6% in overcast condition and 8% in sunny conditions) due to the visibility spectral factor $V(\lambda)$ of the light incoming into the indoor space which is improved by the spectral shifting operated by the LSC component (see Fig. 6).

Furthermore in sunny conditions it is possible to exploit daylighting to reduce electricity needs for artificial lighting whereas in overcast conditions the use of artificial light is often mandatory to reach the illuminance levels required to perform the visual task.

5.4. Experimental measures on color rendering index in sunny sky condition

In sunny sky condition, when direct radiation is preponderant and the effect of the color of the yellow LSC is relevant and can be critical, a focus on color rendering index was performed.

As results it can be underlined as in the model configuration without the light-shelf, the general color render index of the incoming light is reduced by 7% with a value of 90 for the model with LSC integration. The general color render index with the LSC integration is however compatible with the visual task requirements (Table 2). Nevertheless it should be noted that in the picture (Fig. 2) of the physical model with the LSC fanlight where the yellow spot inside the indoor space occurs the visual task can be affect leading to critical values of the R_a.

The color rendering diagrams for the CG and LSC configurations are shown in Figs. 7 and 8.

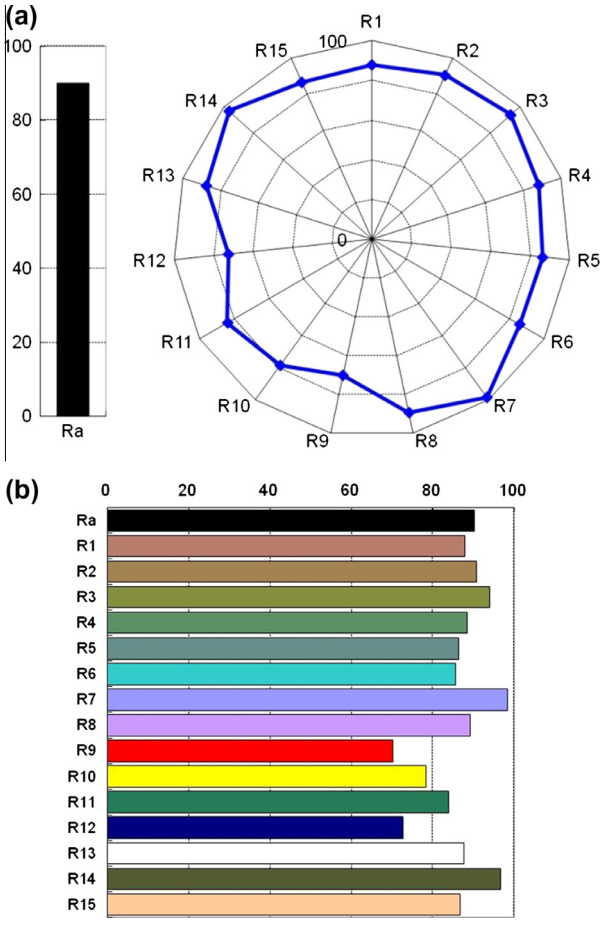

Fig. 8. Color rendering diagram of the scaled physical model with LSC integration (LSC). (For interpretation of the references to colour in this figure legend, the reader is referred to the web version of this article.)

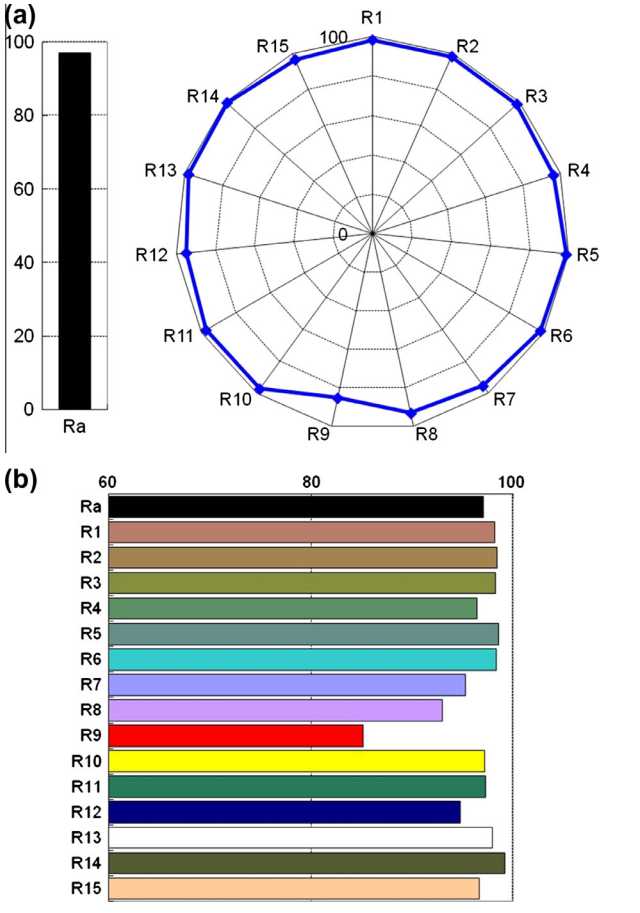

Fig. 9. Color rendering diagram of the light into the scaled physical model with clear glass and light-shelf (CG + LS). (For interpretation of the references to colour in this figure legend, the reader is referred to the web version of this article.)

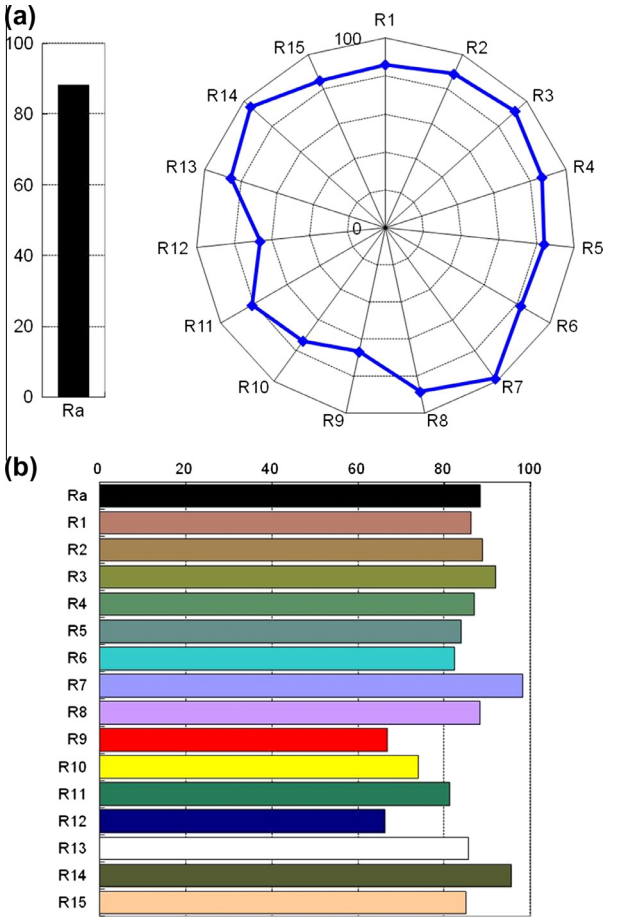

Fig. 10. Color rendering diagram of the light into the scaled physical model with LSC integration and light-shelf (LSC + LS). (For interpretation of the references to colour in this figure legend, the reader is referred to the web version of this article.)

Adding the light-shelf to the glazed façade, the mix of light created by the incoming light from the glazed window and the yellow LSC fanlight changes some special color rendering indexes ($R1$ to $R15$) although the general color rendering index value R_a is 88. Some colors as the red, blue and yellow have values reduced to 80, however compatible with common visual task (Table 2) not strictly related to detailed color identification. The diagrams of color rendering index for the two solutions are shown in Fig. 9 (CG + LS) and Fig. 10 (LSC + LS).

6. Discussion and conclusion

The LSC integration in the building envelope can be useful to produce electricity (Earp et al., 2004; Dienel et al., 2010; Friedman, 1980; Batchelder et al., 1981) and to characterize the envelope through the language of color in the transparent surfaces. Nevertheless the use of color in architecture has to be correctly evaluated because of its potential to change the visual comfort parameters to perform visual task concerned. The yellow LSC component developed by ENI Donegani Institute shifts the light spectrum nearest to the eye visual peak sensitivity wavelength and, when integrated into a glazed façade, affects the incoming light lowering, as mean valuable effect, the correlated color temperature warming the light inside the space producing a stimulating effect (Cuttle and Boyce, 1988; Davis and Ginthner, 1990), a pleasant perception and a mood of relaxing comfort (Vienot et al., 2009; Noguchi and Sakaguchi, 1999). Furthermore the efficacy of the incoming luminous flux, i.e. how many lumen are related to the incident radiant flux (W) is enhanced by the presence of the LSC component with an improvement by 6–8% in every sky condition. Moreover, in sunny sky condition an improvement of illuminance level when direct solar radiation is predominant has been registered. In this condition, however, the illuminance level is high and colored light spots can occur compromising the color rendering of the objects if located in correspondence of the spots. This problem does not happen in overcast sky condition and in any case it can be avoided using sun shading systems to reflect the direct light (e.g. with a light-shelf installation) (Lim et al., 2012). To describe in detail potential issues about visual comfort parameters in the most critical situation, assessment on color rendering index of the light in sunny sky condition have been carried out highlighting that the performance of the yellow LSC component does not change the light up to incompatible values complaining instead the European standard requirement. These results can suggest that the LSC integration is compatible and advantageous in term of visual comfort, however further studies will be carried out on the integration of the LSC in different orientations and portions of the glazed façade, to find sizing thresholds to optimize the effects underlined.

Acknowledgments

The study is based on the analyses carried out on the samples produced by ENI Donegani Institute and the authors would like to thank Dr. Roberto Fusco for the useful discussions and valuable insights while carrying out the present work. Special thanks go to Ludovico Maestri for is valuable contribution in the testing phase.

References

Aste, N., Tagliabue, L.C., Del Pero, C., Testa, D., Fusco, R., 2015. Performance analysis of a large-area luminescent solar concentrator module. Renew. Energy 76, 330–337.

Batchelder, J.S., Zewail, A.H., Cole, T., 1981. Luminescent solar concentrators. 2: Experimental and theoretical analysis of their possible efficiencies. Appl. Opt. 20, 3733.

Bellia, L., Bisegna, F., Spada, G., 2011. Lighting in indoor environments: visual and non-visual effects of light sources with different spectral power distributions. Build. Environ. 46, 1984–1992.

Berson, D.M., Dunn, F.A., Takao, M., 2002. Phototransduction by retinal ganglion cells that set the circadian clock. Science 295, 1070–1073.

Boyce, P.R., Cuttle, C., 1990. Effect of correlated colour temperature on the perception of interiors and colour discrimination. Lighting Res. Technol. 22, 19–36.

Claros, S.T., Soler, A., 2001. Indoor daylight climate-comparison between light shelves and overhang performances in Madrid for hours with unit

sunshine fraction and realistic values of model reflectance. Sol. Energy 71 (4), 233–239.
Claros, S.T., Soler, A., 2002. Indoor daylight climate influence of light shelf and model reflectance on light shelf performance in Madrid for hours with unit sunshine fraction. Build. Environ. 37, 587–598.
Clements-Croome, D.J. 1977. Assessment of the Influence of the Indoor Environment on Job Stress and Productivity of Occupants in Offices. In: Proceedings of Healthy Buildings/IAQ'97, Washington, DC.
Coppedè, C., Palladino, P. 2012. La luce in Architettura. Maggioli Editore.
Cuttle, C., Boyce, P.R., 1988. Kruithof revisited: a study of people's responses to illuminance and color temperature of lighting. Lighting Aust. 8, 17–28.
Dacey, D.M., Liao, H., Peterson, B., Robinson, F., Smith, V., Pokorny, J., Yau, K.-W., Gamlin, P.D., 2005. Melanopsin-expressing ganglion cells in primate retina signal colour and irradiance and project to the LGN. Nature 433, 749–754.
Davis, R.G., Ginthner, D.N., 1990. Correlated color temperature, illuminance level, and the Kruithof curve. J. Illum. Eng. Soc. 19, 27–38.
Debije, M.G., Verbunt, P.P.C., 2012. Thirty years of luminescent solar concentrator research: Solar energy for the built environment. Adv. Energy Mater. 2, 12–35.
Dienel, T., Bauer, C., Dolamic, I., Bruhwiler, D., 2010. Spectral-based analysis of thin film luminescent solar concentrators. Sol. Energy 84, 1366–1369.
Earp, A.A., Smith, G.B., Swift, P.D., Franklin, J., 2004. Maximising the light output of a luminescent solar concentrator. Sol. Energy 76, 655–667.
European Standard EN 12646:2011, Light and lighting – lighting of work places – Part 1: Indoor work places. Comité Européen de Normalisation. CEN/TC 169.
Fadzil, S.F.S., Sia, S.J., 2004. Sunlight control and daylight distribution analysis: the KOMTAR case study. Build. Environ. 39, 713–717. Fekete, J., Sik-Lanyi, C., Schanda, J., 2010. Spectral discomfort glare sensitivity investigations. Ophthal. Physiol. Opt. 30, 182–187. Friedman, P.S. 1980. Calculation of Luminescent Solar Concentrator Efficiencies. LSC Contract Report, Owens-Illinois, SERI Contract XS-9-8216-1.
Gamlin, P.D., McDougal, D.H., Pokorny, J., Smith, V.C., Yau, K.W., Dacey, D.M., 2007. Human and macaque pupil responses driven by melanopsin-containing retinal ganglion cells. Vision Res. 47, 946–954.
Goetzberger, A., 1978. Fluorescent solar energy collectors: operating conditions with diffused light. Appl. Phys. 16, 399.
Goetzberger, A., Greubel, W., 1977. Solar energy conversion with fluorescent collectors. Appl. Phys. 14, 123.
Hattar, S., Liao, H.-W., Takao, M., Berson, D.M., Yau, K.-W., 2002. Melanopsin-containing retinal ganglion cells: architecture, projections, and intrinsic photosensitivity. Science 295, 1065–1070.
Hernandez-Andres, J., Lee Jr., R.L., Romero, J., 1999. Calculating correlated color temperatures across the entire gamut of daylight and skylight chromaticities. Appl. Opt. 38 (27).
Hernandez-Andres, J., Romero, J., Nieves, J.L., 2001. Color and spectral analysis of daylight in southern Europe. J. Opt. Soc. Am. A 18 (6), 1325.
Ju, J., Chen, D., Lin, Y., 2012. Effects of correlated color temperature on spatial brightness perception. Color Res. Appl. 37 (6).
Judd, D.B., MacAdam, D.L., Wyszecki, G., Budde, H.W., Condit, H.R., Henderson, S.T., Simonds, J.L., 1964. Spectral distribution of typical daylight as a function of correlated color temperature. J. Opt. Soc.Am. 54 (8), 1031–1040.
Kim, W., Kim, J.T., 2012. A prediction method to identify the glare source in a window with non-uniform luminance distribution. Energy Build. 46, 132–138.
Li, D.H.W., 2010. A review of daylight illuminance determinations and energy implications. Appl. Energy 87, 2109–2118.
Lim, Y.W., Kandar, M.Z., Ahmad, M.H., Ossen, D.R., Abdullah, A.M., 2012. Building façade design for daylighting quality in typical government office building. Build. Environ. 57, 194–204.
Linhart, F., Scartezzini, J.L., 2011. Evening office lighting e visual comfort vs. energy efficiency vs. performance? Build. Environ. 46, 981–989.
Littlefair, P.J., 1995. Light shelves: computer assessment of daylighting performance. Lighting Res. Technol. 27, 79–91.
Lynn, N., Mohanty, L., Wittkopf, S., 2012. Color rendering properties of semi-transparent thin-film PV modules. Build. Environ. 54, 148–158.
Lutfi Hidayetoglu, M., Yildirim, K., Akalin, A., 2012. The effects of color and light on indoor wayfinding and the evaluation of the perceived environment. J. Environ. Psych. 32, 50–58.
Mills, P.R., Tomkins, S.C., Schlangen, L.J.M., 2007. The effect of high correlated color temperature office lighting on employee wellbeing and work performance. J. Circadian Rhythms 5, 2.
Morita, T., Hirano, Y., Tokura, H., 2003. Temporal variability of preferred lighting conditions self-selected by women. Physiol. Behav. 78, 351–355.
Nazzal, A.A., 2005. A new evaluation method for daylight discomfort glare. Int. J. Ind. Ergon. 35, 295–306.
Noguchi, H., Sakaguchi, T., 1999. Effect of illuminance and color temperature on lowering of physiological activity. Appl. Human Sci. 18, 117–123.
Palladino, P. 2005. Manuale di illuminazione. Tecniche Nuove. Palladino, P. 2002. Lezioni di illuminotecnica. Tecniche Nuove. Petrides, A., Trexler, E.B., 2008. Differential output of the high-sensitivity rod photoreceptor: AII Amacrine Pathway. J. Comp. Neurol. 507, 1653–1662.
Pinto, P.D., Maciel Linhares, J.M., Cardoso Nascimento, S.M., 2008. Correlated color temperature preferred by observers for illumination of artistic paintings. J. Opt. Soc. Am. A 25 (3), 623.
Scudo, P.F., Abbondanza, L., Fusco, R., Caccianotti, L., 2010. Spectral converters and luminescent solar concentrators. Sol. Energy Mater. Sol. Cells 94, 1241–1246.
Shin, J.Y., Yun, G.Y., Kim, J.T., 2012. View types and luminance effects on discomfort glare assessment from windows. Energy Build. 46, 139–145.
Soler, A., Oteiza, P., 1997. Light shelf performance in Madrid. Build. Environ. 32, 87–93.
Swartz, B.A., Cole, T., Zewail, A.H., 1977. Photon trapping and energy transfer in multiple-dye plastic matrices: an efficient solar energy concentrator. Opt. Lett. 1, 73–75.
Tachibanaki, S., Shimauchi-Matsukawa, Y., Arinobu, D., Kawamura, S., 2007. Molecular mechanisms characterizing cone photoresponses. Photochem. Photobiol. 83, 19–26.
Van Bommel, W.J.M., 2006. Non-visual biological effect of lighting and the practical meaning for lighting for work. Appl. Ergon. 37, 461–466.
Van Bommel, W.J.M., Van den Beld, G.J., 2004. Lighting for work: a review of visual and biological effects. Lighting Res. Technol. 36 (4), 255–269.
Van Sark, W.G.J.H.M., 2013. Luminescent solar concentrators – a low cost photovoltaics alternative. Renew. Energy 49, 207–210.
Vienot, F., Durand, M.L., Mahler, E., 2009. Kruithof 's rule revisited using LED illumination. J. Mod. Opt. 56 (13), 1433–1446.
Webb, A.R., 2006. Considerations for lighting in the built environment: non-visual effects of light. Energy Build. 38, 721–727.
Wiegman, J.W.E., Van Der Kolk, E., 2012. Building integrated thin film luminescent solar concentrators: detailed efficiency characterization and light transport modelling. Sol. Energy Mater. Sol. Cells 103, 41–47.